



Syntheses and structures of two new organic–inorganic hybrid lanthanide derivatives based on Keggin-type polyoxometalates

Dehui Li, Bo Sun, Weichen Qi, Jinglei Xiao, Jing Yang & Xiying Han

To cite this article: Dehui Li, Bo Sun, Weichen Qi, Jinglei Xiao, Jing Yang & Xiying Han (2016) Syntheses and structures of two new organic–inorganic hybrid lanthanide derivatives based on Keggin-type polyoxometalates, *Molecular Crystals and Liquid Crystals*, 624:1, 183–189, DOI: 10.1080/15421406.2015.1011479

To link to this article: <http://dx.doi.org/10.1080/15421406.2015.1011479>



View supplementary material [↗](#)



Published online: 11 Feb 2016.



Submit your article to this journal [↗](#)



Article views: 53



View related articles [↗](#)



View Crossmark data [↗](#)

Syntheses and structures of two new organic–inorganic hybrid lanthanide derivatives based on Keggin-type polyoxometalates

Dehui Li, Bo Sun, Weichen Qi, Jinglei Xiao, Jing Yang, and Xiyang Han

School of Pharmaceutical Sciences, Changchun University of Chinese Medicine, Changchun, PR China

ABSTRACT

Two new organic–inorganic hybrid Keggin-type polyoxometalates containing lanthanide(III) cations with 3D supramolecular framework structures, $[\text{La}(\text{DMSO})_8][\text{PW}_{12}\text{O}_{40}]$ (**1**) and $[\text{La}(\text{DMSO})_8][\text{PMo}_{12}\text{O}_{40}]$ (**2**) (DMSO = dimethyl sulfoxide), have been synthesized in aqueous solution under moderate conditions and further characterized by elemental analysis, inductively coupled plasma (ICP) analyses, IR spectroscopy, electronic spectra, thermogravimetric analysis, and single-crystal X-ray diffraction analyses. The title complexes exhibit similar 3D supramolecular frameworks directed by the different hydrogen bonding interactions. The TG curve exhibit the weight loss of complex **1**, which can be divided into five stages, suggesting that the intensity of coordination bonds are different between La(III) and DMSO molecules.

KEYWORDS

Lanthanide derivatives;
Keggin-type; synthesis;
crystal structure; thermal
property

1. Introduction

Lanthanide derivatives of polyoxometalates (LDPOMs) have been attracting increasing attention not only because polyoxometalates (POMs) have potential applications in variety areas such as catalysis, nanotechnology, and sorption [1–5], but also lanthanide (Ln) cations can impart useful functionality such as luminescent, magnetic, or Lewis acid catalytic centers to POMs [6–8]. Therefore, more and more chemists have focused on developing polyoxoanions-based LDPOMs [9–14]. For example, Niu and co-workers prepared two 1D polyoxometalate-based composite complexes derived from the Wells–Dawson subunit $[\{\text{Ce}(\text{DMF})_4(\text{H}_2\text{O})_3\}\{\text{Ce}(\text{DMF})_4(\text{H}_2\text{O})_4\}(\text{P}_2\text{W}_{18}\text{O}_{62})]\cdot\text{H}_2\text{O}$ and $[\{\text{La}(\text{DMF})_6(\text{H}_2\text{O})\}\{\text{La}(\text{DMF})_{4.5}(\text{H}_2\text{O})_{2.5}\}(\text{P}_2\text{W}_{18}\text{O}_{62})]$ (DMF = *N,N'*-dimethylformamide) at room temperature, in which two rare earth coordination cations play diverse roles in the realization of the molecular assemblies of 1D composite compounds [12]. Pope et al. reported the structural characterization of 1D $[\text{Ln}(\alpha\text{-SiW}_{11}\text{O}_{39})(\text{H}_2\text{O})_3]^{5-}$ (Ln = La(III), Ce(III)) complexes, showing that these anions are polymeric in the solid state [15]. However, comparing with the extensive reports of LDPOMs, the saturated Keggin-type LDPOMs are very rare [16–18]. Wang et al. prepared a series of LDPOMs constructed from $[\text{GeMo}_{12}\text{O}_{40}]^{4-}$ polyoxoanions and $[\text{Ln}(\text{N-methyl-2-pyrrolidone})_4(\text{H}_2\text{O})_4]^{3+}$ cations [16]. Niu's group synthesized the Ln-supported 1D polymeric chain structures $[\{\text{Ln}(\text{N-methyl-2-pyrrolidone})_6\}(\text{PMo}_{12}\text{O}_{40})]_n$ (Ln = La, Ce, Pr) [17].

On the basis of the aforementioned points and as a part of continuous efforts towards new LDPOMs based on Keggin-type polyoxoanions and Ln(III) cations in this study, two different Keggin-type polyoxometalates were selected to assemble with La(III) ion and DMSO molecules, aiming at generating new LDPOMs and investigating the influence of polyoxometalates on the formation of high-dimensional supramolecular frameworks. As a result, we have obtained two new La(III) derivatives of polyoxometalates $[\text{La}(\text{DMSO})_8][\text{PW}_{12}\text{O}_{40}]$ (**1**) and $[\text{La}(\text{DMSO})_8][\text{PMo}_{12}\text{O}_{40}]$ (**2**) in aqueous solution under moderate conditions. In addition, the TG-DTA of complex **1** has been studied.

2. Experimental section

2.1. Materials and general methods

All chemicals were used as purchased without further purification. C and H element analyses were performed on a Perkin-Elmer 2400 elemental analyzer; P, W, La were analyzed on a PLASMA-SPEC(I) ICP atomic emission spectrometer. IR spectra were recorded in the range of 400–4000 cm^{-1} on an Alpha Centaur FT/IR spectrophotometer using KBr pellets. Electronic spectra ($\lambda = 190\text{--}350\text{ nm}$) were obtained on a Beckman Du-8B spectrometer in solution. TG-DTA analyses were carried out on the America TA company SDT-2960 instrument in air atmosphere with a heating rate of $10^\circ\text{C min}^{-1}$.

2.2. Preparation of the complexes

2.2.1. Synthesis of $[\text{La}(\text{DMSO})_8][\text{PW}_{12}\text{O}_{40}]$ (**1**)

A solution of 10 mL of $\text{H}_3\text{PW}_{12}\text{O}_{40}$ (0.5 mmol) was added lanthanum nitrate (0.5 mmol) under stirring, which was heated at 90°C in water bath until being dry. Then the dried sample was dissolved in the mixed solvent of acetonitrile and water, subsequently 1 mL DMSO was added dropwise. After 20 minutes, the resulting solution was cooled to room temperature, filtered and left to evaporate at room temperature. One day later, colorless blocks of the title complex, suitable for single-crystal X-ray diffraction analyses, were obtained in 26% yield based on $\text{H}_3\text{PW}_{12}\text{O}_{40}$. Anal. Calcd for $\text{C}_{16}\text{H}_{48}\text{LaO}_{48}\text{PS}_8\text{W}_{12}$: La: 3.82; W: 60.59; C: 5.28; P: 0.85; H: 1.33%; Found: La: 3.78; W: 60.57; C: 5.30; P: 0.82; H: 1.31%.

2.2.2. Synthesis of $[\text{La}(\text{DMSO})_8][\text{PMo}_{12}\text{O}_{40}]$ (**2**)

The preparation of the complex **2** is similar to that of **1**. Replacing $\text{H}_3\text{PW}_{12}\text{O}_{40}$ with $\text{H}_3\text{PMo}_{12}\text{O}_{40}$ leads to the formation of **2**. Yield: 19% based on $\text{H}_3\text{PMo}_{12}\text{O}_{40}$. Anal. Calcd for $\text{C}_{16}\text{H}_{48}\text{LaMo}_{12}\text{O}_{48}\text{PS}_8$: La: 5.37; Mo: 44.52; C: 7.43; P: 1.20; H: 1.87%; Found: La: 5.39; Mo: 44.48; C: 7.48; P: 1.19; H: 1.91%.

2.3. X-ray crystallography

X-ray diffraction data for complexes **1** and **2** were collected on a Bruker SMART APEX II diffractometer equipped with a CCD area detector and graphite-monochromated $\text{Mo K}\alpha$ ($\lambda = 0.71073\text{ \AA}$) by ω and θ scan mode. All of the structures were solved by direct methods and refined on F^2 by full-matrix least-squares methods using the SHELXS program of the SHELXTL package [19]. For complexes **1** and **2**, the crystal parameters, data collection, and refinement results are summarized in Table 1. Selected bond distances and bond angles are listed in Tables S1 and S2. CCDC 227939 and 1021748 for complexes **1** and **2** contain the

Table 1. Crystal and refinement data for complexes **1** and **2**.

Empirical formula	C ₁₆ H ₄₈ LaO ₄₈ PS ₈ W ₁₂	C ₁₆ H ₄₈ LaMo ₁₂ O ₄₈ PS ₈
<i>F</i> _w	3641.10	2586.18
Crystal system	Triclinic	Triclinic
space group	<i>P</i> −1	<i>P</i> −1
<i>a</i> (Å)	11.774(2)	11.794(2)
<i>b</i> (Å)	12.165(2)	12.172(2)
<i>c</i> (Å)	22.981(5)	22.866(5)
α (°)	84.66(3)	84.63(3)
β (°)	82.31(3)	82.32(3)
γ (°)	85.28(3)	85.37(3)
<i>V</i> (Å ³)	3239.9(11)	3231.4(11)
<i>Z</i>	2	2
<i>T</i> (K)	293(2)	293(2)
<i>D</i> _c /g cm ^{−3}	3.732	2.658
<i>F</i> (000)	3232	2464
Goodness-of-fit on <i>F</i> ²	1.031	1.009
Reflections collected	20805	19874
Unique data	14491	12849
<i>R</i> _{int}	0.0742	0.0797
θ Range (°)	0.90–27.48	2.34–27.48
<i>R</i> ₁ [<i>I</i> > 2σ(<i>I</i>)] ^a	0.0736	0.0769
<i>wR</i> ₂ ^b (all data) ^a	0.2072	0.2160

$$^a R_1 = \sum |F_o| - |F_c| / \sum |F_o|;$$

$$^b wR_2 = \sum [w(F_o^2 - F_c^2)^2] / \sum [w(F_o^2)^2]^{1/2}$$

supplementary crystallographic data in this paper. These data can be obtained free of charge from The Cambridge Crystallographic Data Centre via www.ccdc.cam.ac.uk/data_request/cif.

3. Results and discussion

3.1. Description of crystal structures of complexes **1** and **2**

X-ray crystallography shows that complexes **1** and **2** are isostructural, except that the bond distances and angles are slightly different. Thus, the structure of **1** is discussed in detail as an example. The asymmetric structural unit of **1** consists of one discrete [La(DMSO)₈]³⁺ and one [PW₁₂O₄₀]^{3−} polyanion unit. As shown in Fig 1, La1(III) coordination cation is eight-coordinate, adopting a distorted square antiprism geometry with the La1–O distances of 2.42(2)–2.525(16) Å, in which all of O atoms are from the DMSO molecules. In the polyanion unit, the crystallographic disorder more often appeared in many other α-Keggin [PW₁₂O₄₀]^{3−} crystal structures [20–22]. The central P atom is surrounded by a cube of eight oxygen atoms with each oxygen site half occupied. The P–O bonds lengths are in the range of 1.47(2)–1.59(2) Å and the angles of O–P–O are in the range of 62.2(13)–180°, which demonstrates that the PO₄ tetrahedron is distorted. 12 WO₆ octahedral arrange in four W₃O₁₃ of three edged-share octahedral. The groups of W₃O₁₃ are linked by sharing corners with each other to the central PO₄ tetrahedron. All W–W distance are nearly equal, ranging from 3.544 to 3.564 Å (mean 3.554 Å). The angles of W–O_b/O_c–W are also nearly equal, ranging from 138.5 to 142.5°. The crystallographic disorder averages the W–W bond distances and W–O_b/O_c–W angles between M₃ triplets and within M₃ triplets. The W–O_t bonds are in the usual range of 1.637–1.698 Å (mean 1.667 Å), whereas the W–O_b/O_c bonds in all WO₆ octahedral fall into two resolved

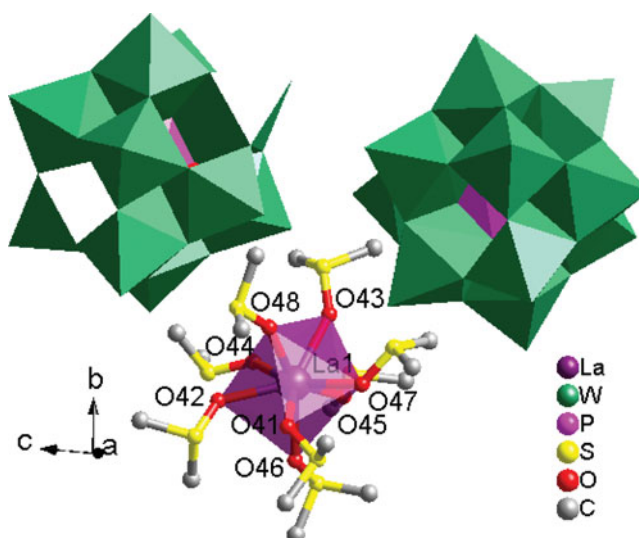


Figure 1. Representation of the molecular structure unit of **1**.

categories, the long pairs of W-O bonds in the range of 1.87–1.95 Å (mean 1.91 Å) and short pairs in the range of 1.85–1.91 Å (mean 1.877 Å).

In the complex, the polyoxoanion and coordination cation are linked up through electrostatic interactions. As shown in Fig. 2, there exist various hydrogen bonding interactions between $[\text{La}(\text{DMSO})_8]^{3+}$ cations and two different kinds of $[\text{PW}_{12}\text{O}_{40}]^{3-}$ polyanions. Two $[\text{La}(\text{DMSO})_8]^{3+}$ cations and one kind of $[\text{PW}_{12}\text{O}_{40}]^{3-}$ polyanion construct a $[\text{La}(\text{DMSO})_8]$ cation circle through C–H...O hydrogen bonding interaction [C10–H10B...O39 = 3.3558(5) Å], which further connects with another kind of $[\text{PW}_{12}\text{O}_{40}]^{3-}$ polyanion by hydrogen bonding interaction [C16–H16B...O11 = 3.3641(7) Å] to form a 1D chain (Fig. 2). And these 1D chains are extend to a 2D double layer (Fig. 3) by hydrogen bond C7–H7B...O4 [3.3639(4) Å]. Finally, the neighboring 2D double layers are joined together through hydrogen bonding interaction [C12–H12A...O29, 3.3476(4) Å] to form a 3D framework, as shown in Fig. 4. In **1**, each $[\text{La}(\text{DMSO})_8]^{3+}$ cation is linked with four $[\text{PW}_{12}\text{O}_{40}]^{3-}$ polyanions, and two kinds of $[\text{PW}_{12}\text{O}_{40}]^{3-}$ polyanion are connected to four $[\text{La}(\text{DMSO})_8]$ cations, respectively. Finally, a (4,4,4)-connected 3D supramolecular network of **1** is formed by the hydrogen bonds between the $[\text{PW}_{12}\text{O}_{40}]^{3-}$ anions and $[\text{La}(\text{DMSO})_8]$ cations (Fig. 5).

3.2. IR spectra of complex 1

Comparing the IR spectrum of complex **1** with that of $\text{H}_3\text{PW}_{12}\text{O}_{40}$ (see Fig. S1), it can be observed that the anion of complex **1** remains Keggin structure: the characteristic peaks at 1080, 979, 893, and 809 cm^{-1} are attributed to $\nu_{\text{as}}(\text{P}-\text{O}_\text{a})$, $\nu_{\text{as}}(\text{W}-\text{O}_\text{t})$, $\nu_{\text{as}}(\text{W}-\text{O}_\text{b}-\text{W})$, and

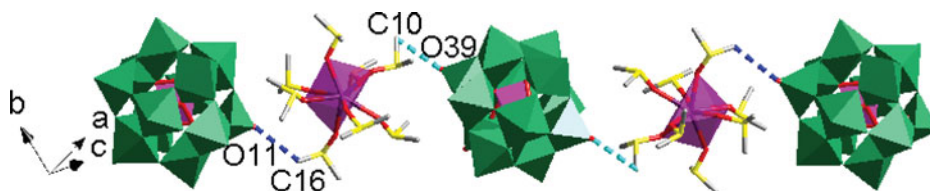


Figure 2. View of the 1D supramolecular chain in **1**.

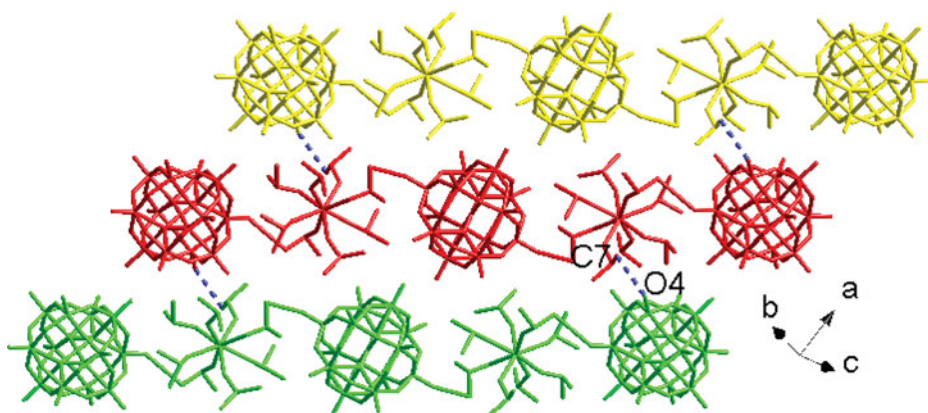


Figure 3. View of the 2D supramolecular layer in **1**.

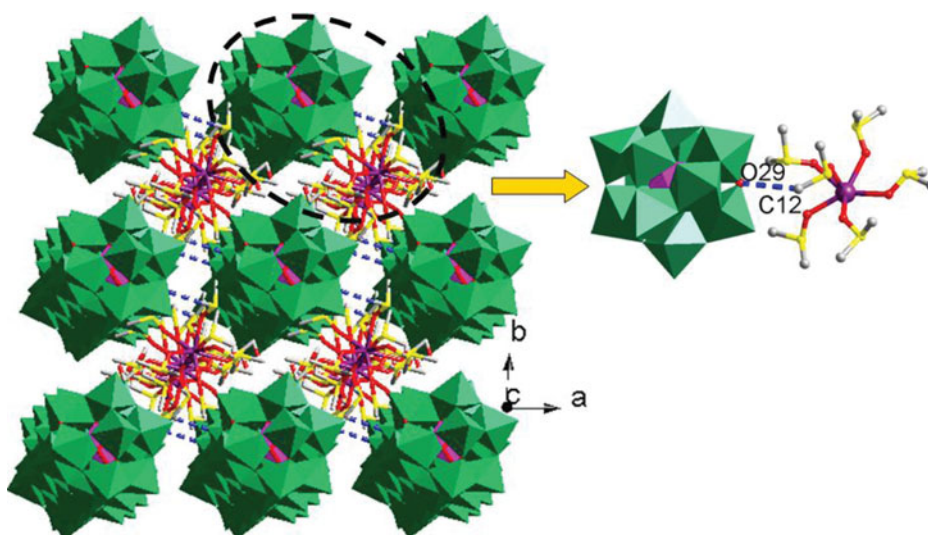


Figure 4. View of the 3D supramolecular framework of **1**.

$\nu_{as}(W-O_c-W)$, respectively. The 3012 and 2919 cm^{-1} features are attributed to vibration of C-H of DMSO, the feature at 1413 cm^{-1} can be assigned to the deformed vibration of C-H of DMSO. The vibrational bond of S=O of DMSO has a red-shift from 1055 cm^{-1} to 1010.11 cm^{-1} , suggesting that DMSO as ligands are coordinating to lanthanum ion by means of their O atoms, which is supported as well by crystal structure data.

3.3. UV spectra of complex **1**

Comparison of the UV spectrum of complex **1** with that of $H_3PW_{12}O_{40}$ (see Fig. S2), obvious difference hasn't been observed. Both have two absorption peaks at 205 and 250 nm that can be assigned to O_t-W , O_b/O_c-W charge-transfer band. This indicates that the interaction between heteropoly anion and lanthanum cation is rather weak in the solution. Though DMSO molecules have absorption at ca. 210 nm, it is covered by the absorption of heteropoly anion.

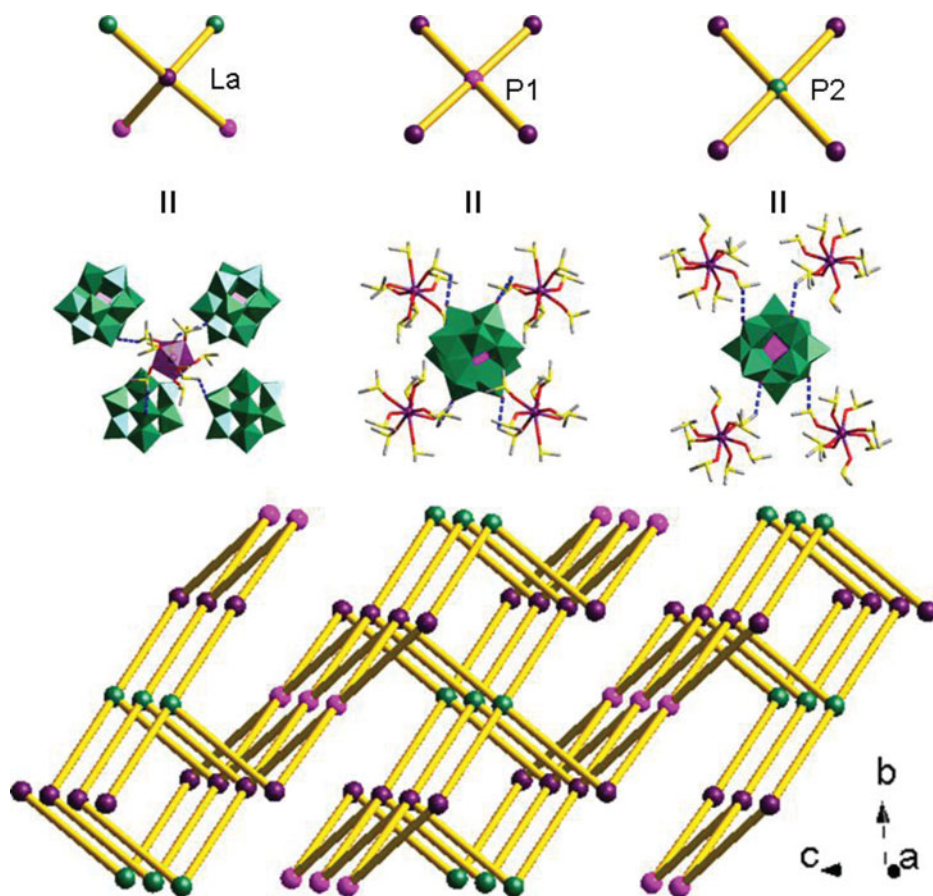


Figure 5. The simplified representation of the 3D supramolecular network of **1**.

3.4. TG-DTA of complex **1**

The thermal properties of complex **1** was studied by thermogravimetric analysis and differential thermal analysis that were determined in the range of 20–1000°C in air. The TG curve is divided into five stages (see Fig. S3). Up to 280°C the first three steps continuously loses weight 8.44%, corresponding to the release of four DMSO molecules; there is one endothermic and four exothermic peaks at 66, 139, 211, 262, 310°C on the DTA curve. The fourth weight loss in the temperature range 310 to 400°C is ca. 6.8% corresponding to the release of three DMSO molecules; there is a strong exothermic peaks at 419.4 °C on the DTA curve, suggesting that DMSO molecules have been drastically oxidized accompanied by the weight loss. The fifth step start from 470°C, and lose weight 1.87%, corresponding to the release of the rest one DMSO molecule. There is a weak endothermic peak at 494 °C on the DTA curve. The whole weight loss (ca.17.11%) is in good agreement with the calculated value (17.16%). The separate losses of DMSO molecules can be attributed to the different intensity of the coordination bonds between DMSO molecules and lanthanum ion, which is as well supported by the crystal structure analysis. As can be seen from Table S1, among the eight La–O interatomic distances, four (2.525 Å, 2.499 Å, 2.495 Å, and 2.494 Å) are longer than others, so they lost first under 280°C; the remainder DMSO molecules lost until the temperature reach 470°C for their short bond (only 2.42 Å).

4. Conclusions

Two new organic–inorganic hybrid lanthanide derivatives based on Keggin-type polyoxometalates with 3D supramolecular framework structures were successfully achieved, and their structures were elucidated by X-ray crystallography. The result of thermal analysis shows that the intensity of coordination bonds is different between DMSO molecules and lanthanum cations. Under similar conditions, many possible novel structure species are very likely to be obtained, which paves the way for further development in the exploration of our synthetic work. Now, we are currently exploring this avenue.

Supplemental data for this article can be accessed at <http://www.tandfonline.com/gmcl>.

References

- [1] Day, V. W., & Klemperer, W. G. (1985). *Science*, 228, 533.
- [2] Bi, Y. F., Wang, X. T., Liao, W. P., Wang, X. F., Wang, X. W., *et al.* (2009). *J. Am. Chem. Soc.*, 131, 11650.
- [3] Hirai, K., Furukawa, S., Kondo, M., Uehara, H., Sakata, O., *et al.* *Angew.* (2011). *Chem. Int. Ed.*, 50, 8057.
- [4] Gassensmith, J. J., Furukawa, H., Smaldone, R. A., Forgan, R. S., Botros, Y. Y., *et al.* (2011). *J. Am. Chem. Soc.*, 133, 15312.
- [5] Sadakiyo, M., Yamada, T., & Kitagawa, H. (2011). *J. Am. Chem. Soc.*, 133, 11050.
- [6] Kortz, U., & Matta, S. (2001) *Inorg. Chem.*, 40, 815.
- [7] Bonchio, M., Bortolini, O., Conte, V., & Sartorel, A. (2003). *Eur. J. Inorg. Chem.*, 42, 699.
- [8] Luo, Q., Howell, R. C., Bartis, J., Dankova, M., Horrocks, W. D., *et al.* (2002). *Inorg. Chem.*, 41, 6112.
- [9] Howell, R. C., Perez, F. G., Jain, S., Horrocks, W. D., Rheingold, A. L., *et al.* (2001). *Angew. Chem. Int. Ed.*, 40, 4031.
- [10] Kido, J., & Okamoto, Y. (2002). *Chem. Rev.*, 102, 2357.
- [11] Zhang, C., Howell, R. C., Scotland, K. B., Perez, F. G., Todaro, L., *et al.* (2004). *Inorg. Chem.*, 43, 7691.
- [12] Niu, J. Y., Guo, D. J., Wang, J. P. & Zhao, J. W. (2004). *Cryst. Growth Des.*, 4, 241.
- [13] Wang, J. P., Zhao, J. W. Y. Duan, X. Y. & Niu, J. Y. (2006). *Cryst. Growth Des.*, 6, 507.
- [14] Wang, J. P., Duan, X. Y., Du, X. D., & Niu, J. Y. (2006). *Cryst. Growth Des.*, 6, 2266.
- [15] Sadakane, M., Dickman, M. H., & Pope, M. T. (2000). *Angew. Chem., Int. Ed.*, 39, 2914.
- [16] Zhang, H., Duan, L. Y., Lan, Y., Wang, E. B. & Hu, C. W. (2003). *Inorg. Chem.*, 42, 8053.
- [17] Niu, J. Y., Wei, M. L., Wang, J. P., & Dang, D. B. (2004). *Eur. J. Inorg. Chem.*, 2004, 160.
- [18] Li, S. Z., Zhang, D. D., Guo, Y. Y., Ma, P. T., Qiu, X. Y., *et al.* (2012). *Dalton Trans.*, 41, 9885.
- [19] Sheldrick, G. M. (2008). *Acta Crystallogr. Sect. A*, 64, 112.
- [20] Han, Q. X., Zhang, L. J., He, C., Niu, J. Y., & Duan, C. Y. (2012). *Inorg. Chem.*, 51, 5118.
- [21] Ma, F. J., Liu, S. X., Sun, C. Y., Liang, D. D., Ren, G. J., *et al.* (2011). *J. Am. Chem. Soc.*, 133, 4178.
- [22] Pang, H. J., Peng, J., Zhang, C. J., Li, Y. G., Zhang, P. P., *et al.*, (2010). *Chem. Commun.*, 46, 5097.